Biomaterials Science

Graphene oxide modified with aptamer-conjugated gold nanoparticles and heparin: a potent targeted anticoagulant

Journal:	*Biomaterials Science*
Manuscript ID:	BM-COM-05-2014-000156.R2
Article Type:	Communication
Date Submitted by the Author:	10-Jul-2014
Complete List of Authors:	So, Yi-Heng; National Taiwan Ocean University, Institute of Bioscience and Biotechnology Chang, Huan-Tsung; National Taiwan University, Chemistry Chiu, Wei-Jane; National Taiwan Ocean University, Institute of Bioscience and Biotechnology Huang, Chih-Ching; National Taiwan Ocean University, Institute of Bioscience and Biotechnology

Biomaterials Science

RSCPublishing

COMMUNICATION

Graphene oxide modified with aptamer-conjugated gold nanoparticles and heparin: a potent targeted anticoagulant

Cite this: DOI: 10.1039/x0xx00000x

Received 00th May 2014,
Accepted 00th May 2014

DOI: 10.1039/x0xx00000x

www.rsc.org/

Yi-Heng So,[a] Huan-Tsung Chang,[b] Wei-Jane Chiu,[a] and Chih-Ching Huang*[acd]

Graphene oxide (GO) modified with 29-mer thrombin-binding-aptamer-conjugated gold nanoparticles (TBA_{29}–Au NPs/GO) can synergistically inhibit the thrombin-mediated cleavage of fibrinogen to fibrin. To further improve anticoagulation efficiency in human plasma, TBA_{29}–Au NPs/heparin/GO has been prepared from TBA_{29}–Au NPs/GO and heparin that can also bind thrombin. The dose-dependence of thrombin clotting time (TCT) delay caused by TBA_{29}–Au NPs/heparin/GO is 21.4, 17.0 and >100 times higher than that caused by the TBA_{29}–Au NPs, TBA_{29}–Au NPs/GO and commercially available drugs (heparin, argatroban, hirudin or warfarin), respectively.

Introduction

Blood coagulation involves a series of enzymatic reactions, largely localized on vascular and cellular surfaces, and results in the formation of a fibrin clot.[1] Thrombin (activated factor II) is a multifunctional serine protease produced by the cleavage of prothrombin at two positions by the factor Xa–involved prothrombinase complex (factor Va, negatively charged phospholipid vesicles, and calcium).[2] Thrombin plays many vital roles in the coagulation cascade, converting soluble fibrinogen into insoluble strands of fibrin, catalyzing many other coagulation–related reactions, including directly such as activating protein C and platelets, and providing feedback amplification of factors V, VIII, XI, and XII.[3] Therefore, thrombin is a very attractive target for anticoagulation factors.

Many specific inhibitors have been used for regulating thrombin activity during surgical procedures and for treating patients with arterial or venous thromboembolisms.[4] Thrombin (which has a molecular weight of 37 kDa) is a heterodimer consisting of two polypeptide chains, A and B. The catalytic domain in thrombin has a deep cleft around its catalytic site and two large electropositive surfaces, called exosite I (the fibrinogen–binding site) and exosite II (the heparin–binding site), on opposite sides of the active site cleft.[5] The biological activity of thrombin is strongly affected by substrates, cofactors, and inhibitors that bind to exosites I and II.[6,7] Many direct thrombin inhibitors, which block the enzymatic active site, are currently available for clinical use, but most of them cause serious side effects and suffer from narrow therapeutic windows due to their low specificity and indirect action.[8,9] Thus, more efficient and specific anticoagulation agents are required for treating coagulation–related cardiovascular diseases. A 15–mer thrombin–binding–aptamer (TBA_{15}) has been shown as a potential anticoagulation drug because it can inhibit the activity of thrombin through its interaction with fibrinogen–binding exosite I.[10] However, TBA_{15} at a high concentration is required to give an appropriate anticoagulant response because of its low binding affinity. Moreover, oligonucleotide aptamers are easily degraded by blood nucleases and has a short lifetime (~2 min) in blood, limiting their potential use.[11] Conjugation of amptamers through phosphorothioate linkages and use of locked-nucleic acids has been shown to be efficient in improving the half-life and binding affinity of aptamers.[12] However, toxicity of the expensive non-natural modified aptamers is a concern.

Recent studies have demonstrated that linearly assembled 15-mer thrombin-binding-aptamer (TBA_{15}) and TBA_{29} (using a poly-dA linker or a polyethylene glycol linker), synthetic dendritic TBAs, and nanostructured TBAs can inhibit thrombin activity efficiently through their multivalent interactions.[13–18] More recently, we have found that TBA_{29}–conjugated gold nanoparticles (TBA_{29}–Au NPs) have a strong anticoagulant potency (82 times stronger than TBA_{29}) because they cause steric blocking and have high binding affinity for thrombin in a biological plasma mimic.[19] In this study, we prepared TBA_{29}–Au NPs functionalzed graphene oxide (GO) nanocomposite (TBA_{29}–Au NPs/GO), with the aim of further improving anticoagulant potency. TBA_{29} is easy folded to a G-quadruplex structure.[20] The TBA_{29}–Au NPs functionalized on graphene oxide GO mainly through the π–π stacking interactions between the square planar guanine tetrad and GO.[21–24] The multivalent TBA_{29} units on Au NPs result in the strong copperative π–π stacking interaction between TBA_{29}–Au NPs and GO. The hydrophobic and the hydrogen bonding interactions between TBA_{29} and GO could not be excluded.[25] TBA_{29}–Au NPs/GO can bind to thrombin effectively to

inhibit the activity of thrombin to catalyze the cleavage of fibrinogen to form fibrin (Scheme 1a). The TBA_{29}–Au NPs/GO in comparison with TBA_{29}–Au NPs provided higher inhibitory potency toward thrombin, mainly because of the synergistic effects of TBA_{29}–Au NPs and GO. The anticoagulant efficiency of TBA_{29}–Au NPs/GO was 3.7 times stronger than that of TBA_{29}–Au NPs in a mimic physiological solution. We found that heparin–modified TBA_{29}–Au NPs/GO (TBA_{29}–Au NPs/heparin/GO; Scheme 1b) had an ultrahigh anticoagulation potency toward thrombin in plasma. We measured the dose–dependence of the thrombin clotting time (TCT) delay, showing that the as-prepared TBA_{29}–Au NPs/heparin/GO had a much stronger anticoagulation potency than that of TBA_{29}–Au NPs/GO and commercially available rugs (heparin, argatroban, hirudin, and warfarin).

Results and Discussion

Preparation and Characterization of TBA_{29}–Au NPs/GO Nanomaterials.

GO was synthesized using an improved Hummers' method from graphite with a particle size of 7–11 μm.[26,27] Transmission electron microscopy (TEM) and atomic force microscopy (AFM) images show that the average size of the single-layer GO is about 400 nm, and the monolayer thickness is about 1.8 nm (Fig. 1a and 1c). From dynamic light scattering (DLS) measurements (Fig. S1), we estimated the hydrodynamic diameters of GO to be ~300 nm with narrow size distribution, indicating the GO were well dispersed in the solution. As-prepared GO (24 mg L^{-1}) and TBA_{29}–Au NPs (0.5 nM; 13 nm) in a sodium phosphate solution (5 mM; pH 7.0) were used to prepare TBA_{29}–Au NPs/GO. About 90% of the TBA_{29}–Au NPs was determined to be adsorbed onto the GO through comparing the absorbance values at 520 nm of the TBA_{29}–Au NPs in standard solution and in the supernatant after centrifugation (at a relative centrifugation force (RCF) of 1500 *g* for 10 min) of the TBA_{29}–Au NPs/GO mixture. Furthermore, the results of agarose gel separation of the mixtures of TBA_{29}–Au NPs (10 nM) and GO (0–600 mg/L) indicated >90% TBA_{29}–Au NPs were loaded on GO when the concentration of GO was higher than 120 mg L^{-1} (Fig. S2, Supporting Information). A TEM image of TBA_{29}–Au NPs/GO (Fig. 1b) reveals that the TBA_{29}–Au NPs were assembled homogeneously on the surfaces of GOs. The AFM (Fig. 1d) and UV–vis absorption spectra of TBA_{29}–Au NPs/GO (Fig. S3, Supporting Information) further confirm that the Au NPs were dispersed (no aggregation) and well-distributed on the surface of each GO.

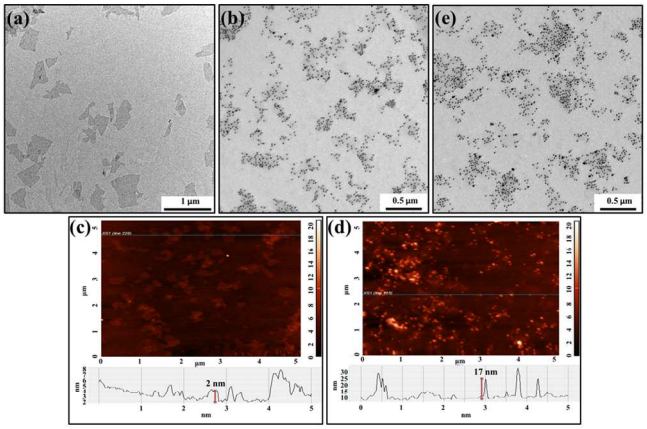

Fig. 1 (a and b) TEM images and (c and d) tapping mode AFM images of (a and c) GO and (b and d) TBA_{29}–Au NPs/GO. (e) TEM image of TBA_{29}–Au NPs/heparin/GO.

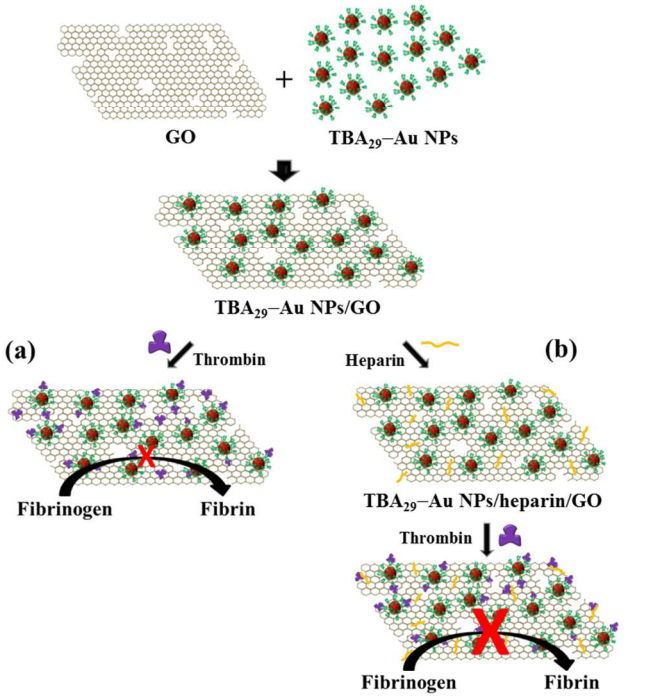

Scheme 1. Schematic of the preparation of (a) graphene oxide (GO) modified with 29-mer thrombin-binding aptamer–conjugated gold nanoparticles (TBA_{29}–Au NPs) and (b) GO modified with TBA_{29}–Au NPs and heparin, showing enhanced inhibitory efficiency toward thrombin.

Effect of TBA_{29}–Au NPs/GO on the Inhibition to Thrombin Activity.

Two well-known TBAs, a 15-mer (TBA_{15}) and a 29-mer (TBA_{29}) were used to prepare TBA-modified AuNPs (TBA–AuNPs) previously and employed to detect and control the activity of thrombin.[28–30] We demonstrated that TBA_{29}–P_8T_{15}–Au NPs (Au NPs conjugated with TBA_{29} with a linker of 15 thymine (T) and 9 stem pairs (P) at the termini of the TBA_{29}) interact strongly with thrombin (K_d<0.01 nM) due to its high local concentration of TBA ligands on the particles' surfaces.[28] In addition, we also demonstrated that 15 thymine units in the linker and 8 stem pairs at the termini of the TBA are important to provide stability and flexibility for strong binding with thrombin.[28] Here, the descriptor "TBA_{29}–Au NPs" was simply used to represent Au NPs conjugated with approximately 70 TBA_{29} units presenting T_{15} and P_8. We tested the inhibitory potencies of TBA_{29}, GO, TBA_{29}–Au NPs, and TBA_{29}–Au NPs/GO by performing typical clotting tests using fibrinogen (1.14 μM), bovine serum albumin (BSA; 100 μM) and thrombin (15 nM) in physiological conditions. The sequences of TBA_{29} and other DNA fragments used in this study are listed in Table S1 (Supporting Information). The real–time coagulation kinetics of thrombin–induced fibrin formation in mimic physiological solution (25 mM tris(hydroxymethyl)aminomethane (Tris)–HCl at pH 7.4, 150 mM NaCl, 5.0 mM KCl, 1.0 mM $MgCl_2$,

and 1.0 mM $CaCl_2$) containing BSA (100 μM) was investigated by measuring the scattered–light intensity caused by fibrin as a function of time (Fig. S4, Supporting Information). The amount of each oligonucleotide present was kept constant (35 nM). Because of the formation of fibrin–gel, the turbidity and light scattering of the reaction mixtures increased with increasing thrombin activity.[29] Through comparing the inhibition potencies of these inhibitors toward thrombin (based on the initial reaction rates, i.e., within 800 s; a high rate reveals a weak inhibitory potency), we found that the potencies decreased in the order TBA_{29}–Au NPs/GO > TBA_{29}–Au NPs > GO > TBA_{29} (Fig. S5, Supporting Information). As controls, the 25–mer random–sequence DNA with T_{15} linker (rDNA, 35 nM), rDNA–modified Au NPs (rDNA–Au NPs), rDNA–Au NPs/GO, and BSA–modified Au NPs (BSA–Au NPs) all provide negligible inhibition toward thrombin (data not shown). We also found that TBA_{15}–Au NPs than TBA_{29}–Au NPs and TBA_{15}–Au NPs/GO than TBA_{29}–Au NPs/GO provided much lower inhibitory abilities, mainly because TBA_{15} than TBA_{29} has a weaker binding affinity for thrombin.[20] Notably, the TBA_{29}–Au NPs/GO inhibition potency (128 cps/sec) was much stronger than that (476 cps/sec) of the TBA_{29}–Au NPs, mainly because of ultrahigh binding ligands present on the surface of GO (Fig. S5, Supporting Information) and/or synergistic effects of TBA_{29}–Au NPs and GO. Compared with free TBA_{29} (K_d ~ 0.5 nM),[20] TBA_{29}–Au NPs/GO had a much higher binding affinity for thrombin ($K_d = 7.0 \times 10^{-12}$ M; Fig. S6, Supporting Information). The binding affinity of TBA_{29}–Au NPs/GO for thrombin was comparable to our previous bivalent TBA_{15}/TBA_{29}–Au NPs ($K_d = 8.86 \times 10^{-12}$).[28] The ultrahigh TBA density on the surface of the Au NPs and TBA_{29}–Au NPs on the surface of GO provided high local concentrations of TBA ligands, enhancing the binding affinity for thrombin.[19,31] In addition, steric blocking and electrostatic interactions between thrombin and GO (zeta potential ~ −45 mV; specific surface area ~2600 m^2/g) could not be excluded for such a strong inhibition. Thrombin activity was strongly inhibited by unmodified 60 mg L^{-1} GO (Fig. S7, Supporting Information) in the absence of background protein (BSA, 100 μM). We believe these synergistic effects (interactions of thrombin with TBA_{29} and with GO, and steric effects) are the main contributors to the ultrahigh inhibitory function of TBA_{29}–Au NPs/GO. Compared to GO covalently modified with oligonucleotides,[32] the preparation of TBA_{29}–Au NPs/GO is relative very simple. Highly dense aptamer molecules could be easily loaded on the GO through multivalent base–graphene pi stacking. When the aptamers were covalently bonded to GO, the aptamer molecules most likely existed as flattened structures, leading to weak affinity toward its targeted molecules. However, the TBA_{29} on the surfaces of the Au NPs/GO provided high flexibility and an appropriate orientation, allowing stronger interaction with thrombin.

Thrombin Clotting Time.

We showed that TBA_{29}–Au NPs/GO had an ultrahigh capacity for inhibiting the activity of thrombin in a mimic biological solution. We further tested its capacity in human plasma samples by performing TCT tests. TCT tests are commonly performed on patients suspected of suffering from coagulopathy and are used to screen for factors I, IIa, and XIII.[33] We first compared the inhibitory potencies of TBA_{29}–Au NPs/GO, TBA_{29}–Au NPs, and commercial anticoagulant drugs, including three direct thrombin inhibitors (heparin, argatroban, and hirudin) and one indirect thrombin inhibitor (warfarin) by performing TCT assays (Fig. 2 and Fig. S8, Supporting Information). The dose–dependence of the TCT delay indicated that the anticoagulation potency of TBA_{29}–Au NPs/GO in plasma was stronger than that of the four commercial drugs, but only slightly stronger than that of the TBA_{29}–Au NPs. The TCT using TBA_{29}–Au NPs/GO ([TBA_{29}] = 8.75 nM) was 87 ± 12 s, which is longer than the TCT in the absence of the inhibitor (20 ± 3 s), whereas the TCTs were 69 ± 8 s, 23 ± 3 s, 21 ± 2 s, 22 ± 4 s, and 21 ± 5 s for TBA_{29}–Au NPs ([TBA_{29}] = 8.75 nM), heparin (8.75 nM), argatroban (8.75 nM), hirudin (8.75 nM), and warfarin (8.75 nM), respectively. We suggest that the nonspecific binding of the plasma proteins to GO weakened the binding strength between TBA_{29}–Au NPs/GO and thrombin.

Heparin–modified TBA_{29}–Au NPs/GO (TBA_{29}–Au NPs/heparin/GO) was prepared (see the experimental section for detailed preparation of TBA_{29}–Au NPs/heparin/GO) to attempt to decrease nonspecific binding and improve the binding affinity. The heparin molecules conjugated with GO probably through multivalent hydrogen bonding and hydrophobic interactions.[34,35] Determination by light scattering experiments revealed about 95% of the heparin was adsorbed onto the GO, through comparing the concentration of heparin in the supernatant after centrifugation of the TBA_{29}–Au

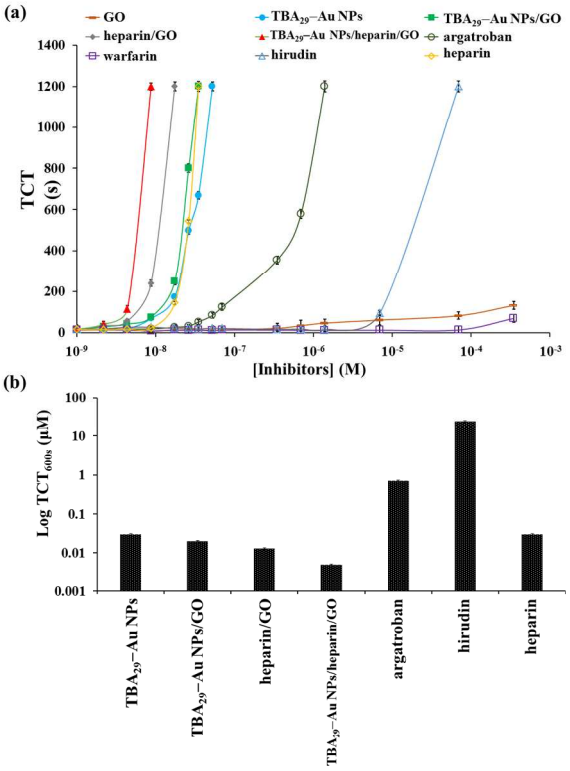

Fig. 2 (a) Dose–dependence of the TCTs using commercial drugs (heparin, argatroban, hirudin, and warfarin) and nanomaterials prepared in this study (GO, TBA_{29}–Au NPs, TBA_{29}–Au NPs/GO, heparin/GO, TBA_{29}–Au NPs/heparin/GO) in human plasma samples. The TCT was taken as the point at which the scattering signal was halfway between the lowest and highest points. The longest time of clotting assays monitored was set at 1200 s. (b) TCT delay to 600 s (TCT_{600s}) of TBA_{29}–Au NPs, TBA_{29}–Au NPs/GO, heparin/GO, TBA_{29}–Au NPs/heparin/GO, argatroban, hirudin, and heparin. The error bars represent the standard deviations of three repeated measurements. Other conditions were the same as those described in Fig. S4.

NPs/heparin/GO mixture to that of control solutions. The heparin did not cause the aggregation of TBA_{29}–Au NPs/GO after heparin adsorbed on GO (Fig. 1e and Fig. S3). We noted the TBA_{29}–Au NPs was not desorbed from the GO after heparin adsorbed on GO from the comparison of absorbance values at 520 nm of the TBA_{29}–Au NPs in standard solution and in the supernatant after centrifugation (at a RCF of 1500 *g* for 10 min) of the TBA_{29}–Au NPs/heparin/GO mixture. The inactivation of thrombin and activated factor X (factor Xa) induced by heparin (a sulfated polysaccharide) is through an antithrombin–dependent mechanism.[36] The inactivation of thrombin by antithrombin III can increase by nearly three orders of magnitude in the presence of heparin. The binding of thrombin to the highly negatively charged heparin appears to be a predominantly electrostatic interaction at a site proximal to the pentasaccharide of the heparin, with an intrinsic K_d of 5–10 μM.[37] The dose–dependence of the TCT delay and TCT delay to 600 s (TCT_{600s}) (Fig. 2) shows that the anticoagulation ability of TBA_{29}–Au NPs/heparin/GO was not only much higher than that of the four commercial drugs but also much higher than that of TBA_{29}–Au NPs/GO, TBA_{29}–Au NPs, and heparin-modified GO (heparin/GO). The TCTs of TBA_{29}–Au NPs/heparin/GO ([TBA_{29}] = 8.75 nM), heparin/GO ([heparin] = 8.75 nM), TBA_{29}–Au NPs/GO ([TBA_{29}] = 8.75 nM), and TBA_{29}–Au NPs ([TBA_{29}] = 8.75 nM) were approximately 75.0, 15.0, 4.4, and 3.5 times longer (t/t_0; t_0 is the TCT in the absence of the inhibitor, and t is the TCT in the presence of the inhibitor), respectively, than that of the TCTs in the absence of any inhibitor (Fig. S9, Supporting Information). The TCT delay caused by TBA_{29}–Au NPs/heparin/GO was 21.4 times higher than that caused by the TBA_{29}–Au NPs and 17.0 times higher than that caused by TBA_{29}–Au NPs/GO. The results clearly show the advantages of using TBA_{29}–Au NPs/heparin/GO over TBA_{29}–Au NPs/GO and TBA_{29}–Au NPs with respect to blood coagulation time. The ultrahigh anticoagulant potency of TBA_{29}–Au NPs/heparin/GO was mainly caused by heparin-passivated GO, decreasing the nonspecific binding between plasma background proteins and GO. In addition, multivalent binding of thrombin with TBA_{29} and heparin molecules also account for enhanced potency. Steric blocking of fibrinogen provided by heparin and TBA_{29}–Au NPs on the GO surfaces cannot be excluded for the obtained stronger inhibitions.

We have further evaluated the anticoagulant capability of TBA_{29}–Au NPs/heparin/GO by the measurement of prothrombin time (PT) and activated partial thromboplastin time (aPTT) in plasma samples. aPTT measurement is a screening test for coagulant factors II, V, VIII, IX, X, XI, and XII of the intrinsic and common pathways, while PT measurement is the test for factors II, V, VII, and X of the extrinsic and common pathways.[38,39] Fig. 3 shows the comparison of elongation of PT and aPPT by TBA_{29}–Au NPs/heparin/GO and four commercial drugs (heparin, argatroban, hirudin, and warfarin). Prolonging the PT and aPTT (t/t_0; t_0 and t are the PT or aPPT in the absence and presence of inhibitor, respectively) in plasma samples by TBA_{29}–Au NPs/heparin/GO, heparin, argatroban, hirudin, and warfarin led to values of 5.9/3.9, 1.5/1.2, 1.0/1.1, 1.1/1.0, and 1.0/1.0 times, respectively. The results further clearly demonstrate the advantages of our TBA_{29}–Au NPs/heparin/GO over commercial drugs with respect to blood coagulation time.

Stability of TBA_{29}–Au NPs/heparin/GO.

First, we study the long-term stability of TBA_{29}–Au NPs/heparin/GO in physiological buffer by DLS measurements. The

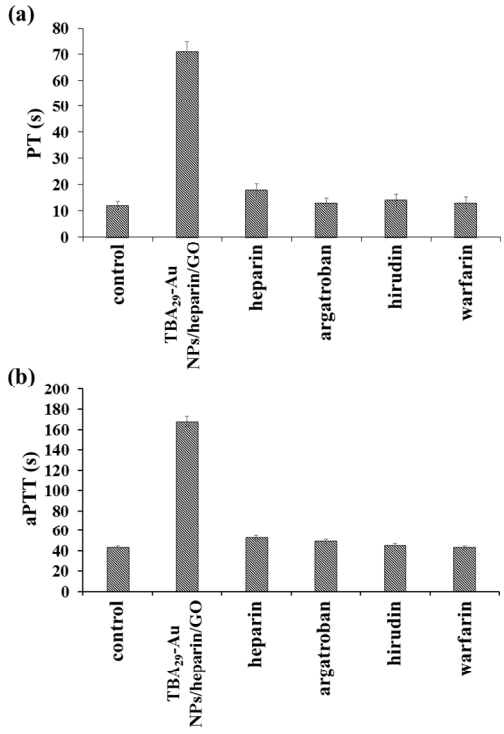

Fig. 3 (a) PT and (b) aPTT measurements, comparison of the anticoagulant potency of TBA_{29}–Au NPs/heparin/GO and four commercial drugs (heparin, argatroban, hirudin, and warfarin) in human plasma. The concentrations of TBA_{29} or commercial drugs in PT and aPPT assays were 105 nM and 35 nM, respectively. To calculate PT and aPTT, the end time was chosen to be the point where the scattering signal reached half-way between the lowest and maximum points. Other conditions were the same as those described in Fig. 2.

DLS results indicated the TBA_{29}–Au NPs/heparin/GO solution was stable (no aggregation) for at least two months when stored in in physiological buffer (Fig. S1d, Supporting Information). The stability of nucleic acids toward nucleases also is an important factor that affects their therapeutic and diagnostic applications.[12,40,41] A major problem with therapeutic oligonucleotide aptamers is their short plasma half–lives, typically of only a few minutes, which usually do not allow time for a sufficient amount of oligonucleotide drug to be delivered to the target site. Prolonging the plasma half–life is a prerequisite for the potential clinical use of a number of drug candidates. We found that the TCT delay for TBA_{29}–Au NPs/heparin/GO was almost constant after 72 h of incubation in the presence of human plasma (Fig. S10, Supporting Information), revealing the TBA_{29}–AuNPs and heparin did not release from GO in plasma. Therefore, we suggest the bleeding risk from the releasing heparin is quite low because the anticoagulation inhibitory potency of TBA_{29}–Au NPs/heparin/GO is >100-fold higher than free heparin (Fig. 2). It has been suggested that high local salt concentrations in the highly negatively charged TBA_{29}–Au NPs/heparin/GO causes increased resistance to nuclease digestion in plasma.[30,42] In addition, the steric blocking of nuclease from accessing TBA molecules, caused by heparin molecules, also contributed to the ultrahigh stability of TBA_{29}–Au NPs/heparin/GO in the plasma samples. Nanoparticles smaller than 10 nm will be rapidly cleared by the kidneys; hence, the TBA_{29}–Au NPs/heparin/GO particles larger than 10 nm shall have lower renal clearance rates.[43] In addition it has

been demonstrated that GO nanosheets exhibited long blood circulation time and low uptake in reticuloendothelial system even if its sizes larger than 100-nm when compared with other carbon nanomaterials.[44] The extraordinary stability of TBA_{29}–Au NPs/heparin/GO suggests that our newly developed anticoagulant may have a long plasma half-life. The small sized GO may be employed for loading of TBA_{29}–Au NPs and heparin if the TBA_{29}–Au NPs/heparin/GO are easy to uptake in reticuloendothelial system in animal studies in future.[45,46]

Biocompatibility of TBA_{29}–Au NPs/heparin/GO.

Recent reports suggest aptamer–modified Au NPs has good biocompatibility for mammalian cells.[47] Although GO could cause some rupture to cell membrane, most studies report mammalian cell viabilities decrease lesser than 20% after exposure to GO concentrations and lower than 10 mg L^{-1} during 24 h or longer.[48] The cytotoxicity of TBA_{29}–Au NPs/heparin/GO towards mammalian cells was evaluated using an Alamar Blue assay. After 24 h of incubation of human embryonic kidney cells (293T cell line) and breast adenocarcinoma cells (MDA–MB–231 and MCF–7 cell lines) with the TBA_{29}–Au NPs/heparin/GO ([GO] = 0–24 mg L^{-1}) , we found that the TBA_{29}–Au NPs/heparin/GO had little influence on cells viability (Fig. S11, Supporting Information). Therefore, we suggest the TBA_{29}–Au NPs/heparin/GO have good biocompatibility toward mammalian cells, considering the TBA_{29}–Au NPs/heparin/GO at the concentration of 24 mg L^{-1} (GO) show ultrahigh inhibitory ability to thrombin in plasma (Fig. 2). Similar to TBA_{29}–Au NPs/heparin/GO, TBA_{29}–Au NPs/GO had little influence on cells viability when the concentration was lower than 24 mg L^{-1} (data not shown). The TBA_{29}–Au NPs/heparin/GO and TBA_{29}–Au NPs/GO show very low cytotoxicity in selected human cell lines probably due to the GO surfaces passivated by high biocompatible aptamer molecules.

We futher studied the *in vitro* hemolysis of TBA_{29}–Au NPs/heparin/GO to verify the satisfactory biocompatibility of TBA_{29}–Au NPs/heparin/GO. The hemolysis assay was performed in defibrinated blood (human) to test the rupture of red blood cells (RBCs) to withstand swelling in contact with TBA_{29}–Au NPs/heparin/GO solution. The hemolysis of RBCs were not observed after incubation with TBA_{29}–Au NPs/heparin/GO solution at 37 °C for 4 h (Fig. S12, Supporting Information), revealing that the TBA_{29}–Au NPs/heparin/GO could serve as a potentially safe anticogulant–nanomaterials. The TBA_{29}–Au NPs/heparin/GO exhibit insignificant cytotoxicity to the mammalian cells and hemolysis insinuate the emergence of this nanocomposite as a future putative anticoagulation drug. However, acute and chronic studies using animal models in the future should be conducted to ensure the potential of TBA_{29}–Au NPs/heparin/GO as a viable drug.

Conclusions

We synthesized a nanocomposite TBA_{29}–Au NPs/heparin/GO which acts as a highly effective anticoagulant through controlling the thrombin activity towards fibrinogen. Such a high anticoagulant activity could be due to i) the high selectivity of TBA_{29} towards thrombin helps heparin to easily access the target and the anticoagulant activity of heparin leads to the inhibition of thrombin activity, and ii) the steric hindrance caused by the TBA_{29}–Au NPs to thrombin, minimizing the access of fibrinogen to the active sites of thrombin. More importantly, the easily prepared and highly active TBA_{29}–Au NPs/heparin/GO is an efficient anticoagulant in human plasma, showing its potential for treating coagulation–related cardiovascular diseases. Furthermore, the *in vitro* cytotoxicity and hemolysis experiment results show that TBA_{29}–Au NPs/heparin/GO has low cytotoxicity and hemolysis effect, revealing that the TBA_{29}–Au NPs/heparin/GO could serve as a potentially safe anticoagulant. In addition, this study shows that GO modified with nanomaterials may be useful for regulating molecular function, controlling protein and DNA binding, and manipulating enzyme activities.

ACKNOWLEDGMENT

This study was supported by the National Science Council of Taiwan under contracts NSC 101-2628-M-019-001-MY3, 102-2113-M-019-001-MY3, and 102-2627-M-019-001-MY3.

Notes and references

[a] Institute of Bioscience and Biotechnology National Taiwan Ocean University, Keelung, 20224, Taiwan; Fax: 011-886-2-2462-2320; Tel: 011-886-2-2462-2192 ext. 5517; E-mail: huanging@ntou.edu.tw

[b] Department of Chemistry, National Taiwan University, Taipei, 10617, Taiwan.

[c] Center of Excellence for the Oceans, National Taiwan Ocean University, Keelung, 20224, Taiwan

[d] School of Pharmacy, College of Pharmacy, Kaohsiung Medical University, Kaohsiung, 80708, Taiwan

† Electronic Supplementary Information (ESI) available: DNA sequences, size measurements by DLS, gel separations, UV–vis absorption of TBA_{29}–Au NPs/GO, initial coagulation reaction rates, plots for calculating the dissociation constant K_d, inhibition of thrombin by unmodified graphene oxide, representative scattering intensity as a function of time, dose-dependent delay in the TCT (t/t_0), stability of TBA_{29}–Au NPs/GO/heparin in plasma, cytotoxicity and hemolysis assays. See DOI: 10.1039/c000000x/

1. K. A. Tanaka, N. S. Key and J. H. Levy, *Anesth. Analg.*, 2009, **108**, 1433.
2. M. S. Chatterjee, W. S. Denney, H. Jing and S. L. Diamond, *Plos Comput. Biol.*, 2010, **6**, e1000950.
3. A. S. Wolberg and R. A. Campbell, *Transfus. Apher. Sci.*, 2008, **38**, 15.
4. S. Yates, and R. Sarode, *Curr. Opin. Hematol.*, 2013, **20**, 552.
5. R. C. Becker and F. A. Spencer, *J. Thromb. Thrombolysis*, 1998, **5**, 215.
6. H. Nar, *Trends. Pharmacol. Sci.*, 2012, **33**, 279.
7. A. Y. Mehta, Y. Jin and U. R. Desai, *Expert. Opin. Ther. Pat.*, 2014, **24**, 47.
8. E. Schaden and S. A. Kozek-Langenecker, *Intensive. Care. Med.*, 2010, **36**, 1127.
9. D. A. Garcia, T. P. Baglin, J. I. Weitz and M. M. Samama, *Chest*, 2012, **141**, 24.
10. K. Padmanabhan, K. P. Padmanabhan, J. D. Ferrara, J. E. Sadler and A. Tulinsky, *J. Biol. Chem.*, 1993, **268**, 17651.

11. I. V. Gribkova, V. A. Spiridonov, A. S. Gorbatenko, S. S. Denisov, F. I. Ataullakhanov and E. I. Sinauridze, *Blood Coagul. Fibrinolysis*, 2014, **25**, 39.
12. A. Avino, C. Fabrega, M. Tintore and R. Eritja, *Curr. Pharm. Des.*, 2012, **18**, 2036.
13. F. Rohrbach, M. I. Fatthalla, T. Kupper, B. Pötzsch, J. Müller, M. Petersen, E. B. Pedersen and G. Mayer, *ChemBioChem*, 2012, **13**, 631.
14. Y. Kim, D. M. Dennis, T. Morey, L. Yang and W. Tan, *Chem. Asian J.*, 2010, **5**, 56.
15. A. Rangnekar, A. M. Zhang, S. S. Li, K M. Bompiani, M. N. Hansen, K. V. Gothelf, B. A. Sullenger and T. H. LaBean, *Nanomedicine*, 2012, **8**, 673.
16. N. S. Petrera, A. R. Stafford, B. A. Leslie, C. A. Kretz, J. C. Fredenburgh and J. I. Weitz, *J. Biol. Chem.*, 2009, **284**, 20620.
17. Y. Kim, Cao Z and W. Tan, *Proc. Natl. Acad. Sci. U. S. A.*, 2008, **105**, 5664.
18. D. Musumeci and D. Montesarchio, *Pharmacol. Ther.*, 2012, **136**, 202.
19. Y.-C. Shiang, C.-C. Huang, T.-H. Wang, C.-W. Chien and H.-T. Chang, *Adv. Funct. Mater.*, 2010, **20**, 3175.
20. D. M. Tasset, M. F. Kubik and W. Steiner, *J. Mol. Biol.*, 1997, **272**, 688.
21. J. Liu, *Phys. Chem. Chem. Phys.*, 2012, **14**, 10485.
22. L. Tang, Y. Wang, Y. Liu and J. Li, *ACS Nano*, 2011, **5**, 3817.
23. F. Li, H. Pei, L. Wang, J. Lu, J. Gao ,B. Jiang, X. Zhao and C. Fan, *Adv. Funct. Mater.*, 2013, **23**, 4140.
24. P. J. Huang and J. Liu, *Small*, 2012, **8**, 977.
25. S. Akca, A. Foroughi, D. Frochtzwajg and H. W. Ch. Postma, *PLoS One*, 2011, **6**, e18442.
26. D. C. Marcano, D. V. Kosynkin, J. M. Berlin, A. Sinitskii, Z. Sun, A. Slesarev, L. B. Alemany, W. Lu and J. M. Tour, *ACS Nano*, 2010, **4**, 4806.
27. W. S. Hummers Jr. and R. E. Offeman, *J. Am. Chem. Soc.*, 1958, **80**, 1339.
28. C.-L. Hsu, S.-C. Wei, J.-W. Jian, H.-T. Chang, W.-H. Chen and C.-C. Huang, *RSC Adv.*, 2012, **2**, 1577.
29. C.-L. Hsu, H.-T. Chang, C.-T. Chen, S.-C. Wei, Y.-C. Shiang and C.-C. Huang, *Chem. Eur. J.*, 2011, **17**, 10994.
30. Y.-C. Shiang, C.-L. Hsu, C.-C. Huang and H-T. Chang, *Angew. Chem. Int. Ed. Engl.*, 2011, **123**, 7802.
31. C. Zhang, J. Ma, J. Yang, S. Liu and J. Xu, *Anal. Chem.*, 2013, **85**, 11973.
32. V. Georgakilas, M. Otyepka, A. B. Bourlinos, V. Chandra, N. Kim, K. C. Kemp, P. Hobza, R. Zboril and K. S. Kim, *Chem Rev.*, 2012, **112**, 6156.
33. V. Ignjatovic, *Methods Mol. Biol.*, 2013, **992**, 131.
34. D. Y. Lee, Z. Khatun, J. H. Lee, Y. K. Lee and I. In, *Biomacromolecules*, 2011, **12**, 336.
35. Y. Wang, P. Zhang, C. F. Liu, L. Zhan, Y. F. Lia and C. Z. Huang, *RSC Adv.*, 2012, **2**, 2322.
36. R. D. Rosenberg, *Am. J. Med.*, 1989, **87**, 2.
37. J. P. Sheehan and J. E. Sadler, *Proc. Natl. Acad. Sci. U. S. A.*, 1994, **91**, 5518.
38. E. Ejlersen, T. Melsen, J. Ingerslev, R. B. Andreasen and H. Vilstrup, *Scand. J. Gastroenterol.*, 2001, **36**, 1081.
39. R. D. Langdell, R. H. Wagner and K. M. Brinkhous, *J. Lab. Clin. Med.*, 1953, **41**, 637.
40. R. E. Wang, H. Wu, Y. Niu and J. Cai, *Curr. Med. Chem.*, 2011, **18**, 4126.
41. M. A. Campbell and J. Wengel, *Chem. Soc. Rev.*, 2011, **40**, 5680.
42. D. S. Seferos, A. E. Prigodich, D. A. Giljohann, P. C. Patel and C. A. Mirkin, *Nano Lett.*, 2009, **9**, 308.
43. B. Wang, X. He, Z. Zhang, Y. Zhao and W. Feng, *Acc. Chem. Res.*, 2013, **46**, 761.
44. X. Zhang, J. Yin, C. Peng, W. Hu, Z. Zhu, W. Li, Q. Fan and Q. Huang, *Carbon*, 2011, **49**, 986.
45. J. T. Robinson, S. M. Tabakman, Y. Liang, H. Wang, H. S. Casalongue, D. Vinh and H. Dai, *J. Am. Chem. Soc.*, 2011, **133**, 6825.
46. H. Zhang, C. Peng, J. Yang, M. Lv, R. Liu, D. He, C. Fan and Q. Huang, *ACS Appl. Mater. Interfaces* 2013, **5**, 1761.
47. L. Yang, X. Zhang, M. Ye, J. Jiang, R. Yang, T. Fu, Y. Chen, K. Wang, C. Liu and W. Tan, *Adv Drug Deliv Rev.*, 2011, **63**, 1361.
48. A. M. Pinto, I. C. Gonçalves and F. D. Magalhães, *Colloids Surf., B*, 2013, **111**, 188.

graphical and textual abstract:

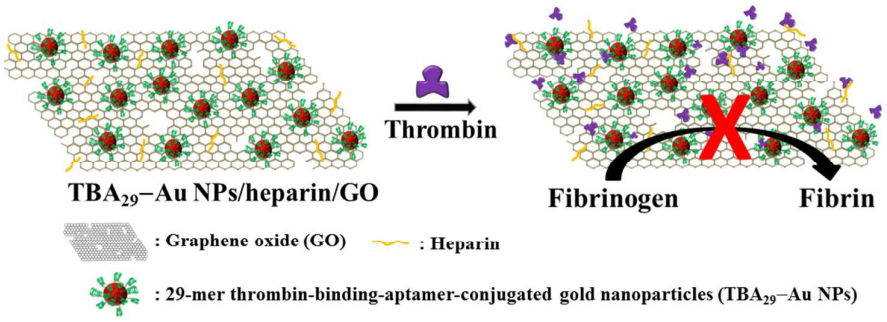

Synthesis of a nanocomposite of aptamer-conjugated gold nanoparticles and heparin co-immobilized graphene oxide acts as a highly effective anticoagulant through controlling the thrombin activity towards fibrinogen.